Heliyon 10 (2024) e29701

Contents lists available at ScienceDirect

Heliyon

journal homepage: www.cell.com/heliyon

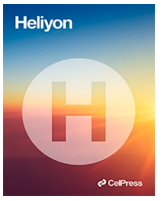

Research article

Characterization of a novel circular bacteriocin from *Bacillus velezensis* 1-3, and its mode of action against *Listeria monocytogenes*

Jun Zhang [a,b], Lihong Zhao [a], Wei Tang [a,c], Jiaxin Li [a], Tao Tang [a,c], Xiaowen Sun [a,b], Xiaoni Qiao [a,b], Zengguo He [a,b,c,*]

[a] *School of Medicine and Pharmacy, Ocean University of China, Qingdao, 266003, China*
[b] *Qingdao Bioantai Biotechnology Co., Ltd., Qingdao, 266071, China*
[c] *Marine Biomedical Research Institute of Qingdao, Qingdao, 266000, China*

ARTICLE INFO

Keywords:
Bacillus velezensis
Circular bacteriocin
Listeria monocytogenes
velezin

ABSTRACT

In this study, isolate *Bacillus velezensis*1-3 was selected out for its anti- Listeria potency, from which a novel circular bacteriocin, velezin, was purified out of the fermentate, and then characterized. Facilitated with a broad antibacterial spectrum, velezin has demonstrated decent inhibitive activity against of foodborne pathogen *L. monocytogenes* ATCC 19115. It exerted the antibacterial activity through damaging the membrane integrity of targeted cell and causing leakage of vital elements, including K^+ ion. It was noteworthy that velezin also inhibited the biofilm formation by *L. monocytogenes* ATCC 19115. At the challenge of velezin, *L. monocytogenes* ATCC 19115 up-regulated expression of genes associated with membrane, ion transporters, stressing-related proteins as well as the genes responsible for the synthesis of small molecule. Taken together, velezin may have potential to be a candidate as natural additive used in food/feed in the future.

1. Introduction

Listeria monocytogenes is the most famous pathogen that leads to foodborne listeriosis [1]. Although the number of cases of listeriosis is small, the derived death rate (as high as 20–30 %) associated with this infection caused makes it a significant public health concern [1,2]. Even with the well-established knowledge and matured expertise in good manufacturing practice and hygienic design, *L. monocytogenes* persists as a recurring food contamination problem in recent years [2]. At present, it is still a real challenge for the food industries to combat the foodborne pathogens like *L. monocytogenes*, thanks to the bug's built-in tolerance to adverse environmental conditions, such as extreme temperatures (as low as 1 °C), acidic pH condition (at pH 2.3), as well as to the formation of resistant biofilms the bug developed in niches it sticks around [2–4]. The need of safe yet natural antibacterial agents against *L. monocytogenes* is on rising.

Bacteriocins are a group of antibacterial peptides with potential against spoilage and pathogenic foodborne bacteria [5,6]. In general, bacteriocins inhibit pathogens by targeting bacterial cell membrane, via a mode different from traditional antibiotics [6]. The proteinaceous nature together with their unique mode of action have evoked considerable interests on bacteriocins for the use in food

* Corresponding author.
E-mail addresses: zhangjun841013@aliyun.com (J. Zhang), zhaolihong1990@163.com (L. Zhao), tianti_121@163.com (W. Tang), hi_jiaxin@163.com (J. Li), 21023424@qq.com (T. Tang), 22545971@qq.com (X. Sun), qiaoxiaoni@stu.ouc.edu.cn (X. Qiao), bioantai88@vip.163.com (Z. He).

https://doi.org/10.1016/j.heliyon.2024.e29701
Received 14 May 2023; Received in revised form 10 April 2024; Accepted 14 April 2024
Available online 22 April 2024

industries as bio-preservatives [7]. Some bacteriocins have already been put into use for food bio-preservation for decades [6–8]. Nisin, the most well-known bacteriocin, has been used as bio-preservative for the control of foodborne pathogens including *L. monocytogenes* [9]. However, limited by its stringency to acidic conditions, nisin has not been used extensively in food particularly those with neutral and or alkaline pH [10]. Therefore, bacteriocins, particularly those that function well under broader pH ranges, is still in demanding.

The circular bacteriocins are a unique group of bacteriocins with decent potential for use as bio-preservatives, thanks to their closed and circular structural characteristics [10–12]. This group of bacteriocins is clustered based on their distinct yet conserved circular peptide backbone arising from the covalent linkage between the N- and C-terminal amino acid residues [11–13]. The most remarkable property of circular bacteriocins is their superior stability compared to their linear counterparts [13]. It is noteworthy that a few circular bacteriocins have demonstrated potential for control of foodborne pathogens, thanks to their decent features such as stability, broad pH adaptability, etc [10–14]. Compared with the large number of linear bacteriocins documented, thus far only 17 circular bacteriocins have been found [15]. Among them, enterocin AS-48, the first discovered circular bacteriocin, has approached near commercial use in food for the control of foodborne pathogens including *L. monocytogenes* [16]. Thus, continuous hunting for new circular bacteriocin may shed light on the exploration of novel arsenal against *L. monocytogenes*.

Previously, in anti- *Listeria* agents screening, an isolate, *Bacillus velezensis* 1-3, was selected out for its potency in coproducing lipopeptides together with an unknow bacteriocins against *L. monocytogenes* [17]. In current study, we reported the discovery a novel circular bacteriocin by *B. velezensis* 1-3. The bacteriocin was isolated, purified and then structural-elucidated, with its physicochemical properties characterized and its mechanism of action pinpointed, respectively. Furthermore, additional studies were conducted to reveal the possible way of resistance developed by *L. monocytogenes*.

2. Materials and methods

2.1. Materials

L. monocytogenes ATCC 19115 was purchased from Ningbo Mingzhou Biotechnology Co., Ltd (Ningbo, China). *Vibrio parahaemolyticus* ATCC17802 was derived from Guangdong Microbial Culture Collection Center (Guangzhou, China). And *Enterococcus faecalis* CICC 21605 was obtained in China Center of Industrial Culture Collection (Beijing, China). All other chemicals and reagents were of analytical grade and are from the sources commercially available.

2.2. Bacterial strains and cultivation

B. velezensis 1-3, the bacteriocinogenic strain, was isolated from a sample provided by local dentistry clinics [17]. All

Table 1
Antimicrobial spectrum of velezin.

Strains	Source	Medium and temperature (°C)	Antibacterial spectrum
Gram-positive bacteria			
L. monocytogenes	ATCC 19115	TSB-YE, 37 °C	+++
E. faecalis	CICC21605	MRS, 37 °C	++
S. aureus	screened in our lab	MH, 37 °C	++
S. sciuri	screened in our lab	MH, 37 °C	+
S. epidermidis	screened in our lab	MH, 37 °C	+
S. lentus	screened in our lab	MH, 37 °C	++
B. cereus	screened in our lab	MH, 37 °C	+
Gram-negative bacteria			
P. aeruginosa	screened in our lab	MH, 37 °C	–
V. parahaemolyticus	ATCC17802	MH, 37 °C	–
V. cholerae	screened in our lab	MH, 37 °C	–
V. alginolyticus	screened in our lab	MH, 37 °C	–
A. hydrophila	screened in our lab	MH, 37 °C	–
E. coli	screened in our lab	MH, 37 °C	+
E. cloacae	screened in our lab	MH, 37 °C	
C. sakazakii	screened in our lab	MH, 37 °C	+
K. pneumoniae	screened in our lab	MH, 37 °C	–
A. haemolyticus	screened in our lab	MH, 37 °C	+
Fungi			
C. albicans	screened in our lab	YPD, 28 °C	++
R. solani	screened in our lab	PDA, 28 °C	+
A. versicolor	screened in our lab	PDA, 28 °C	++

The diameter of the Oxford cup was 0.6 cm.
(+) Indicating the diameter of inhibition zone ≤0.6 cm.
(++) Indicating the diameter of inhibition zone >0.6 cm and ≤1.2 cm.
(+++) Indicating the diameter of inhibition zone >1.2 cm.
(−)Indicating no antibacterial activity observed.

microorganisms and culture conditions were listed in Table 1 and *L. monocytogenes* ATCC 19115 was used as the indicator strain for antimicrobial assays.

Seed culture was prepared by adding a single colony of *B. velezensis* 1-3 into 10 mL Tryptic Soy Both supplemented with 0.5 % (w/v) of yeast extract (TSB-YE) in a 50 mL flask, it was then incubated at 37 °C in a rotating shaker at 180 r/min overnight. Then the culture was used to inoculate a 5-liter flask with 1-liter TSB-YE broth followed by shaking at 180 r/min and 37 °C for 24 h. Every 4 h, 1 mL fermentation medium was sampled and centrifuged at 10, 000×*g* for 10 min at 4 °C.

2.3. Tricine-SDS-PAGE and spot-on-lawn

The antimicrobial assay was performed using the agar diffusion method and each sample was subjected to Tricine-SDS-PAGE analysis [18]. Antimicrobial activities of the bands on electrophoresis gel were determined by the spot-on-lawn method [19]. After frozen-drying, supernatants of the fermentates was subjected to Tricine-SDS-PAGE. The gel strip of the sample at harvest was cut and washed by 50 mL aliquots of distilled water, 25 % isopropanol+10 % acetic acid, 2 % Triton X-100, and sterile water, successively. Then the washed strip was placed in sterile Petri dish, and overlaid with 20 mL soft tempered agar (0.8 %) that was inoculated with 200 μL fresh subculture of the indicator strain. The plate was then incubated at 37 °C overnight for inhibition zone observation.

2.4. Purification and identification of the velezin

Bacteriocin velezin was isolated and purified through ammonium sulfate precipitation (AS) followed by gel filtration chromatography [20]. The cells were spin down at 10, 000×*g* for 10 min at 4 °C and ammonium sulfate was added to the fermentation supernatant to precipitate the bacteriocin. The precipitation was re-suspended and then desalted using dialysis bag (1, 000 MWCO, Solarbio, China), and then lyophilized. The derived desalted powder was further separated by Seplife G-50 gel (Sunresin, China) filtration chromatography. The active fractions were collected and lyophilized, and their antibacterial activities were rechecked. The active powder derived herein defined as the antimicrobial crude extract (CE). After check its purity by Tricine-SDS-PAGE, CE was re-desalted by Ziptip C18 and mixed with α-cyano-4-hydroxycinnamic acid (CHCA) for MALDI-TOF/TOF (Brucker, Germany).

2.5. RNA sequencing analysis

The RNA of *B. velezensis* 1-3 extraction was performed using the total RNA isolation kit for bacteria (Songon, China). The ribo-off rRNA depletion kit (Songon, China) was used to remove bacterial rRNA. A cDNA library was generated using the VAHTS™ stranded mRNA-seq library prep kit (Songon, China). The integrity of the RNA was analyzed with Illumina Hiseq™. The quality of raw data was verified using the FastQC program. Mapping of raw sequence reads was performed using the Bowtie2. Annotation of the bacteriocin gene were conducted using NR, GO, COG, and KEGG database. Transcript abundance was calculated using the method of TPM (transcripts per million) in featureCounts software.

The velezin gene was cloned from the genome of *B. velezensis* 1-3. The structural information of velezin was predicted by a series of bioinformatics tools. The signal sequence was analyzed using SignalP-5.0 program (https://services.healthtech.dtu.dk/service.php?SignalP-5.0). The characteristics of primary and tertiary structure of velezin was calculated and predicted by ProtParam (https://web.expasy.org/protparam/) and AlphaFold2 (v2.2.0) program, respectively. The predicted structure of velezin was analyzed by PDB viewer 4.1 software.

2.6. Antibacterial spectrum and MIC values of velezin

An array of indicator strains (Table 1) was used to determine the antibacterial spectrum of velezin by the Oxford cup method [18]. The minimum inhibitory concentration (MIC) of velezin against *L. monocytogenes* ATCC 19115 was determined using the broth microdilution method. Briefly, the purified velezin was 2-fold serially diluted with phosphate buffer (pH 7.0, 0.1 M), then 10 μL diluted solution was added to 90 μL TSB-YE medium which containing approximately 1×10^5 CFU/mL indicator strains in 96-well plates, and the mixture was incubated at 37 °C for 24 h. The antibacterial activity of velezin was tested over a range of 256, 128, 64, 32, 16, 8, 4, 2, 1, 0.5, 0.25, and 0.125 μg/mL, and all assays were performed in triplicate. MIC was defined as the lowest concentration of velezin that inhibited the indicator growth with no visible microbial growth observed.

2.7. Assays on hemolytic and cytotoxic potentials of velezin

Hemolytic potential of velezin to mouse erythrocytes was assayed by following the standardized method [20]. Briefly, 50 μL aliquots of velezin stocks was mixed with 450 μL of 2 % mouse erythrocyte solution (diluted in 0.85 % NaCl), to allow the final concentration of velezin reaching at 2–512 μg/mL, respectively, then the mixtures were incubated at 37 °C for 1 h followed. NaCl at 0.85 % and Triton X-100 at 2 % were used as the negative and positive controls, respectively. Then the derived supernatants were measured at 540 nm by microplate reader. All assays were performed in triplicate. The hemolysis percentages of velezin were calculated by the following equation: Hemolysis (%) = $[(A_t - A_0)/(A_{100} - A_0)] \times 100$ %. A_t was testing absorbances, A_0 was negative absorbance, and A_{100} was positive absorbance.

Resazurin assay was used to evaluate the cytotoxic potential of velezin to human colorectal adenocarcinoma (Caco-2) cells *in vitro* [20]. The Caco-2 cells line was obtained from ATCC (Rockville, MD, USA), ATCC® Number: HTB-37. Cells (4×10^3 cells/well) were

added into 96-well plates in 100 μL Dulbecco's Modified Eagle Medium supplemented with 10 % FBS and incubated at 37 °C for 24 h in 5 % CO_2. Then the broth was replaced with 100 μL fresh medium containing varied amounts of velezin to reach final concentrations set at 2, 4, 8, 32, 128 μg/mL, respectively, followed by incubation for another 24 h. Fresh medium was used as the control. Finally, the resazurin solution (1 mg/mL) was added to each well allowing staining for 4 h. The absorbance of each well was read in a microplate reader at 570 nm. The cell viability was calculated by the equation: Survival rate (%) = ($A_{velezin}/A_{control}$) × 100 %.

2.8. Stability tests on velezin

To evaluate the thermal stability of velezin, the peptide (10 μg/mL in phosphate buffer) was challenged by incubating over a range of temperatures at 20, 40, 60, 80, and 100 °C for 10 min, respectively. The pH stability of velezin was evaluated by incubating velezin solutions (10 μg/mL) at 37 °C at different pH settings for 1 h by using the following buffers: glycine-HCl buffer (pH 2.0), citric acid buffer (pH 4.0), phosphate buffer (pH 6.0 and 8.0), and glycine-NaOH buffer (pH 10.0). The proteolytic-enzyme resistance tests were performed by mixing velezin stock (at 10 μg/mL) with a panel of enzymes including trypsin, papain, pepsin, chymotrypsin and protease K solutions (in phosphate buffer, pH 6.0) at 37 °C for 4 h. The residual antibacterial activities of velezin in the tests aforementioned were determined by the Oxford cup method assay using *L. monocytogenes* ATCC 19115 as the indicator [18].

2.9. Effect of velezin on biofilm formation

The turbidity-measurement based method was applied to study the effect of velezin against biofilm formation by *L. monocytogenes* ATCC 19115 [21]. First, velezin stock solutions were mixed with *L. monocytogenes* ATCC 19115 at 10^6 CFU/mL to reach final concentrations of velezin at 2, 4 and 8 μg/mL, respectively, then the mix were cultured at 37 °C for 24 h in microplate wells. Same volume of phosphate buffer (pH 7.0) and sodium lactate were used as negative and positive controls, respectively. Then, the liquid containing the planktonic bacteria was removed and the microplate wells were gently washed twice with phosphate buffer. Next, the wells were stained with 0.1 % crystal violet solution for 30 min, and the excess dye was rinsed off with phosphate buffer. Finally, the dye absorbed and retained by biofilm was eluted by 95 % ethanol, the derived solution was measured at 570 nm with a microplate reader (BioTek, Winooski, VT, USA). All assays were performed in triplicate.

2.10. Inhibition pattern of velezin

The inhibition pattern of velezin against *L. monocytogenes* ATCC 19115 was determined *in vitro* [22]. In brief, the indicator was cultivated to an OD_{600} approximately at 0.4, and then diluted to 10^6 CFU/mL with fresh TSB-YE medium. Velezin was added to the culture at a final concentration of 1 × , 2 × and 4 × MIC, respectively; sterile water was used as negative control. Then the cultures were incubated at 37 °C and180 r/min. Aliquots of 500 μL of the cultures at 0, 2, 4, 8, and 12 h were taken for colony counting. All assays were performed in triplicate.

2.11. Scanning electron microscopy (SEM) and transmission electron microscopy (TEM) observations

SEM was applied to observe the morphological change of the indicator cells that were challenged with velezin. Indicator cells in the inhibition zone was horizontally cut off the agar plate into 1–2 mm slices. Then, the slices were dehydrated with 30 %, 50 %, 70 %, 85 %, 90 % and 100 % alcohol solutions, respectively. Dried with CO_2, the samples surface was sputter-coated with gold. The specimens were examined by scanning electron microscopy (JSM-6390LV, JEOL, Japan).

For TEM observation, the velezin-challenged bacteria were washed off from the inhibition zone with phosphate buffer. The cells were harvested by centrifugation at 3, 000×*g* for 10 min, then fixed with 100 μL (2.5 % *v/v*) glutaraldehyde at 4 °C overnight, and the fixed cells were re-suspended in the same volume of saline solution. The morphological features of the bacteria were examined with TEM (JEM-2000FX, Hitachi, Japan) at an operating voltage of 80 kV.

2.12. Inner membrane permeability assay

The effect of velezin on the inner membrane permeabilization was conducted by the propidium iodide and acridine orange (PI/AO) uptake assay [23]. Indicator strain was cultured to the value of OD_{600} approximately 0.4, and diluted to 1 × 10^5 CFU/mL with fresh TSB-YE medium. The cultured cells were treated with 1 × MIC, 2 × MIC, and 4 × MIC velezin at 37 °C for 2 h, respectively. Then the harvested cells were washed and re-suspended in phosphate buffer (pH 7.0), and then incubated with PI/AO (10 μg/mL) at 37 °C for 15 min. The fluorescence responses of the stained cells were observed under an inverted fluorescence microscope (Olympus, Japan).

2.13. Determination of K^+ efflux

Indicator strain was cultured to OD_{600} approximately at 0.4 in TSB-YE medium. Cells were collected by centrifugation (at 5, 000×*g* for 10 min), and washed three times with saline (0.85 %), then the pellet was re-suspended in the same volume of saline. The re-suspension was mixed with velezin stock to a final concentration of 1 × MIC, 2 × MIC, 4 × MIC, respectively, and the mixes were incubated at 37 °C. Samples were withdrawn at 0, 5, 10, 30, and 60 min of incubation, respectively. Aliquots were collected by centrifugation at 5, 000×*g* for 10 min to spin down the cells. The supernatant was filtered through 0.22 μm filter and K^+ levels were

examined using atomic absorption spectrophotometer (Shimadzu, Japan). Culture without velezin was used as the control. A standard curve was made using gradient concentrations (0–5 mg/L) of Potassium Standard for Ion Chromatography (Sigma-Aldrich, USA).

2.14. Response of L. monocytogenes ATCC 19115 to sub-MIC of velezin

The indicator strain *L. monocytogenes* ATCC 19115 was sub-cultured to 10 mL TSB-YE broth in 50 mL flask allowing growth to an OD_{600} value of approximately at 0.4. Then 300 μL of the culture was added to 30 mL TSB-YE medium with velezin added to make a final concentration at 0.5 × MIC (in 150 mL flask). The culture without velezin was set as a control. The mixtures were shaken at 180 r/min and 37 °C for 5 h. Then the cells were harvested for RNA isolation, library construction, sequencing, as well as for transcriptomic analysis as aforementioned.

2.15. Statistical analysis

The results were analyzed by one-way ANOVA using SPSS 25.0 software (IBM, USA). Values were considered significantly different at $p < 0.05$.

3. Results and discussion

3.1. Purification and identification of velezin

Bacillus sp. are well known for the potential in producing antibacterial substances producing bacteria, and several bacteriocins were identified from different bacilli isolates as reported elsewhere [6,8,19]. Previously, in the fermentate of *B. velezensis* 1-3, we isolated and identified 3 surfactin lipopeptides together with an unknown antimicrobial [17]. In this study, through Tricine-SDS-PAGE of the fermentate sample, an anti-Listeria peptide (~7 kDa) was identified, and its bacteriocin-like feature was verified by the derived clear inhibition zone against *L. monocytogenes* ATCC 19115 via the simultaneous bioautography assay conducted (Fig. 1A and B). Hereafter the new identified peptide was defined as velezin.

In order to isolate velezin, the pooled fermentate of *B. velezensis* 1-3, AS was added to the supernatant to 30 % saturation to obtain the crude peptide precipitation (Fig. 2A). The precipitation was desalted, and subjected to size-exclusive separation to get the CE of velezin (Fig. 2B). Tricine-SDS-PAGE analysis showed that the CE contained the very ~7 kDa antibacterial peptide band corresponding to that of velezin. MALDI-TOF/TOF MS analysis indicated that the target peptide band in CE had a molecular size of 7, 351.405 Da (Fig. 3). And its putative amino acid sequence was deducted through the further secondary mass spectrometry analysis (Supplementary Fig. S1). Taken together, the strain 1-3 could coproduce bacteriocin and lipopeptide under the conditions applied in this work. Interestingly, the coproduction of bacteriocin and lipopeptide was well documented by *Paenibacillus polymyxa* OSY-DF [19], but the phenomenon has not been reported for *B. velezensis* thus far.

3.2. Transcriptome and bioinformatics analysis

Transcriptome analysis was conducted to seek the structure gene information of velezin from *B. velezensis* 1-3. Total among the 3, 894 gene sequences obtained, a circular bacteriocin gene was annotated with transcript abundance of 348.85. The total length of the gene was 309 bp with 103 amino acid residues encoded. A signal peptide of 29 amino acid residues was identified at the N- terminal of the pro-peptide (Supplementary Fig. S2), behind it was located the core peptide containing 74 amino acid residues. Based on the calculation by the AA sequencing using ProtParam tool, the mass of mature velezin was theoretically calculated to be 7, 369.63 Da,

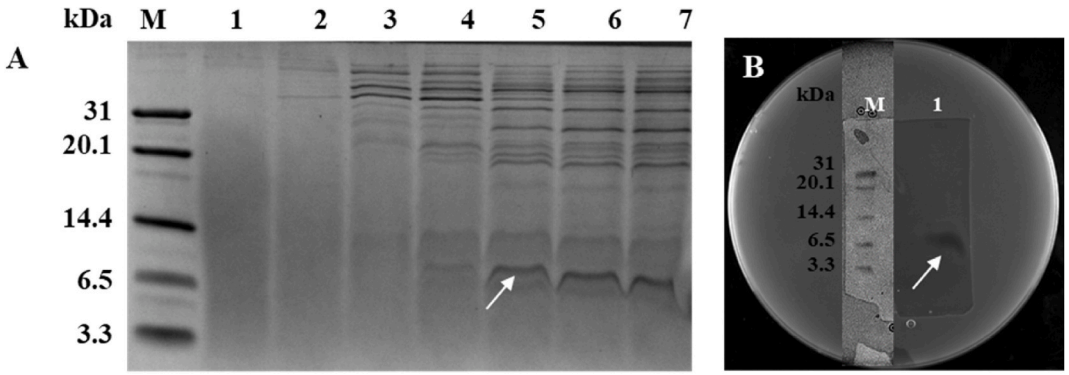

Fig. 1. Expression and activity of the velezin form *B. velezensis* 1-3. (A) Tricine-SDS-PAGE of the fermentation supernatants. Lane 1–7 indicated fermentation supernatants of *B. velezensis* 1-3 taken at 0, 4, 8, 12, 16, 20, and 24 h, respectively. (B) Antibacterial bioautography analysis of the band on Tricine-SDS-PAGE of the 24 h fermentation supernatant. M: marker imaging in natural light; 1: 24 h sample imaging in UV light.

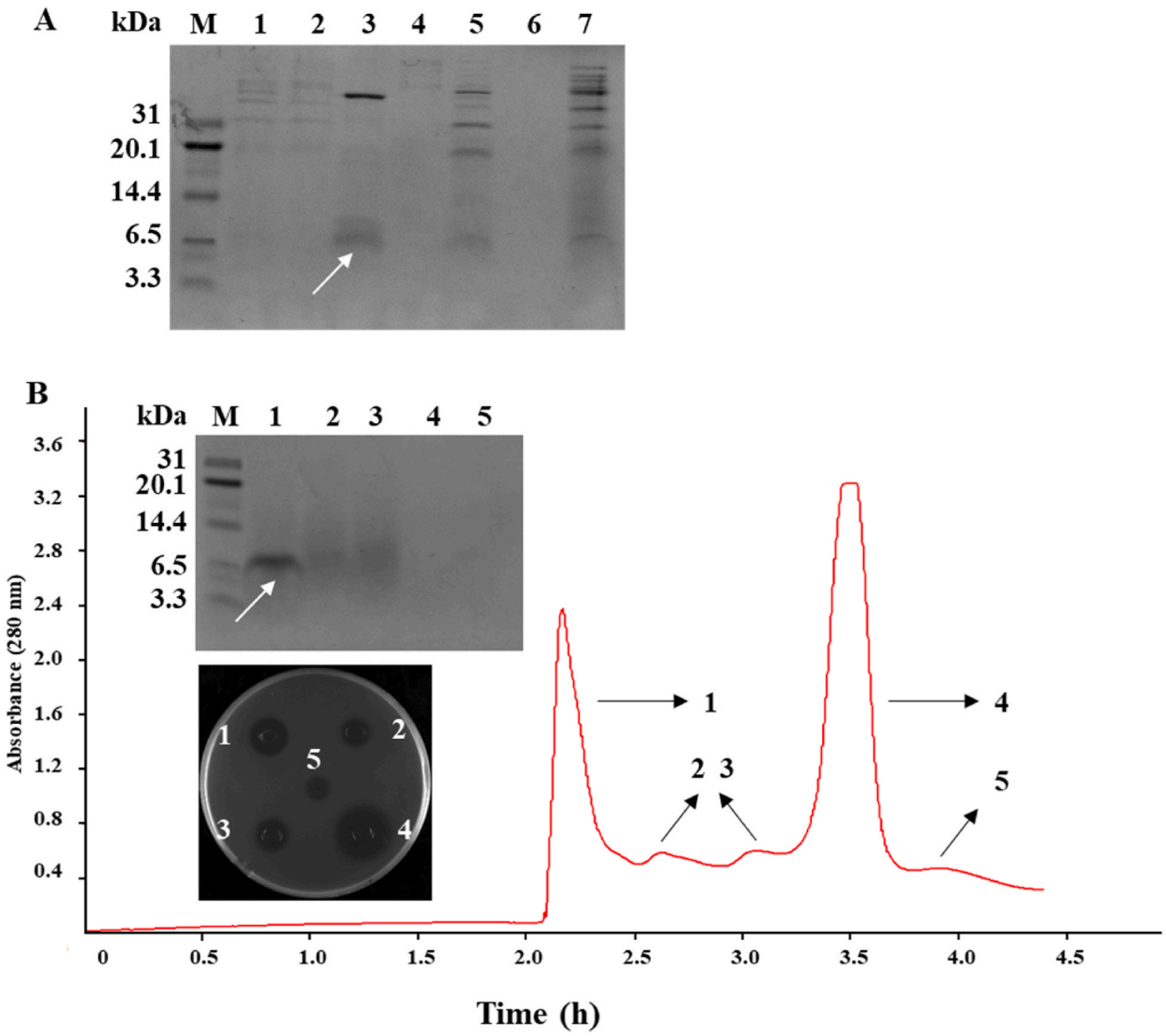

Fig. 2. Purification of the velezin form *B. velezensis* 1-3 CFS. (A) Tricine-SDS-PAGE of AS precipitation: M, marker; lane 1–7 indicated the CFS, 30 % supernatants, 30 % sediment, 60 % supernatants, 60 % sediment, 90 % supernatants, and 90 % sediment, respectively (Most of the antibacterial active substances and 7 kD band were precipitated under 30 % of AS). (B) Purification of the velezin by gel filtration chromatography: M, marker; 1–5 indicated elution parts at different time points. The ~7 kD band with antibacterial active was detected in fraction1 by Tricine-SDS-PAGE and Oxford cup method. And the fraction 4 with antibacterial activity was the lipopeptides surfactin [18].

higher than the mass measurement of 7, 351.405 Da obtained by MALDI-TOF/TOF MS (Fig. 3). A gap of 18.225 Da, just the very size of H_2O, was observed, which was similar to the cases of other circular bacteriocins studies that exemplified the determination of occurrence of circularization marked by the loss of one molecule of water through aligning the gene based mass calculations with the mass measurements obtained through Mass Spectra analyses [24,25]. It was thus assumed that the MW gap of one H_2O as aforementioned could also be explained by the circularization reaction taking place through the condensation of NH–H and CO–OH located at the N- and C-terminal amino acid residues of velezin, respectively.

AlphaFold2 (v2.2.0) program was applied to obtain the three-dimensional structure features of velezin. The predication results indicated that velezin contained up to five α-helices structures (Fig. 4A). It was found that amino acids involved in formation of helixes varied when different amino acids served as the N- and C-terminal for predication (Supplementary Fig. S3). For circular bacteriocins, a conserved structural motif known as saposin fold, existed in the documented ones [26]. And it has been well recognized that the saposin fold motif-like structural conformation was crucial to the antibacterial activities of a panel of circular bacteriocins. Furthermore, saposin fold motif-like conformation has also been acknowledged as the structural foundation that facilitates circular bacteriocins with the superior stabilities against thermal stress, pH variation and the resistance to degradation by proteolytic enzymes, compared to those linear bacteriocins [11,13,26]. In this study, it was noticed that the typical saposin fold conformation was also

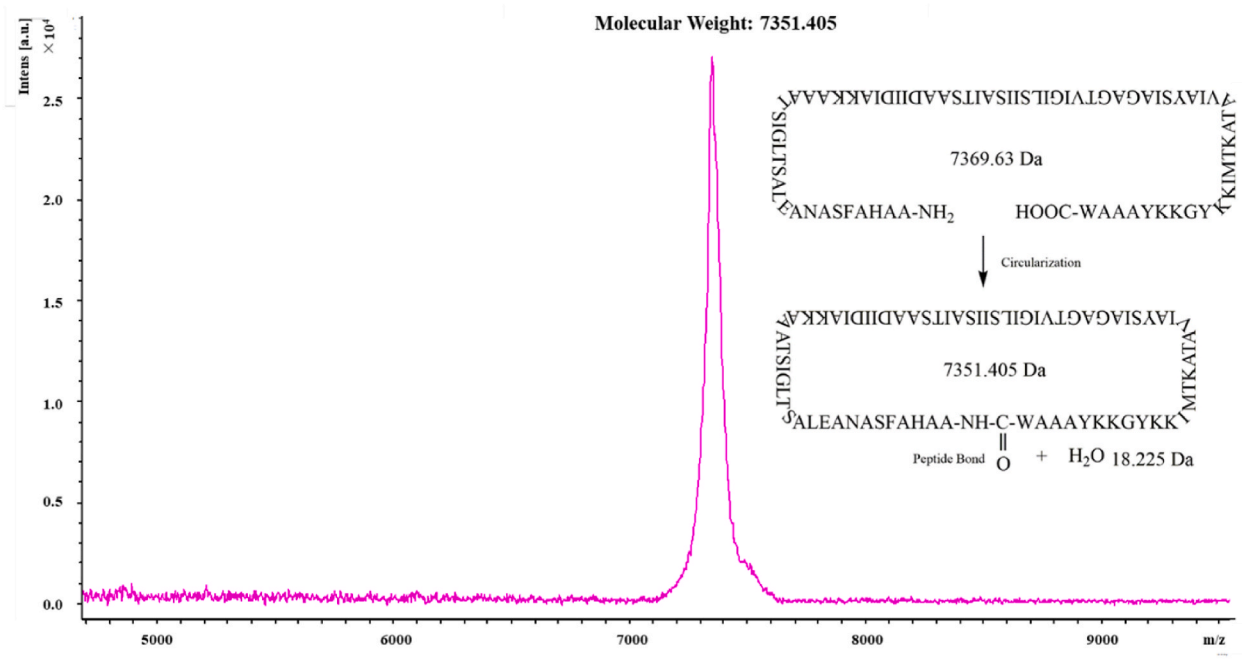

Fig. 3. MALDI-TOF/TOF MS of purified velezin. The molecular weight of velezin was 7351.405 Da.

observed in velezin. It was arranged by four amphipathic α-helices in a distinctly compact architecture, with a small hydrophobic core formed inside (Fig. 4B). Although most of the hydrophobic amino acid residues situated inward in the hydrophobic core of velezin, there were yet several hydrophobic residues exposed at the surface of the spherical structure and formed the hydrophobic patches (Fig. 4B). This type of conformation has been also documented in other circular bacteriocins [26,27,28]. The hydrophobic patches may enable the formation of circular bacteriocin dimers. As have been found in enterocin AS-48, two of these superficial hydrophobic patches allows the dimmer formation through hydrophobic interaction and orientation of two hydrophobic patches [27]. Actually, the region with clustered positive charge is essential for circular bacteriocins to exert antibacterial activity [13]. For velezin, up to seven lysine residues were found, four of them positioned and clustered superficially to form a prominent positive charge region at the surface of the peptide (Fig. 4C). Just as documented with circular bacteriocins carnocyclin A and enterocin NKR-5-3B, the positive charge region was crucial for the circular bacteriocins to bind and anchor to the negative charge area on the membrane of the target strains [11,26,29].

In order to pinpoint gene clusters encoding velezin, *in silico* analysis was conducted by using BAGEL4 online program. Among 40 open reading frames (ORF) identified in the genome, 15 ORF were detected by RNA-seq (Table 2) (Supplementary Fig. S4). In addition to velezin gene, an uncharacterized membrane protein (ORF14) was identified with the highest transcript abundance, and it was assumed to be involved in the across membrane transportation of velezin. Another two genes possibly involved in transport, ABC transporter (ORF 30 and 31) and YutK protein (ORF13), were also found in RNA-seq. Genes similar to both were also reported as transport genes for other circular bacteriocins [13]. However, the gene, involved in self-immunity of velezin was not found in the transcriptome. In fact, there are very limited homology among circular bacteriocin immunity proteins have been documented in known ones, even those that are involved in immunity against bacteriocins of the same class [28]. Despite the easy identification of the gene clusters involved in the biosynthesis of circular bacteriocins, the genes for leader peptides cleavage and followed peptide circularization have not been clearly defined yet thus far [11–13]. Interestingly, in the gene cluster of velezin one gene that encoded an uncharacterized peptidase was found in RNA-seq analysis. In fact, it was reported that some peptidase could enable the enzymatic circularization of the targeted peptides [30,31]. It was thus presumed that the uncharacterized peptidase aforementioned may be involved in the circularization of velezin. To clarify the functionality of the uncharacterized peptidase identified, direct experimental evidence such as gene knock-out approaches is needed [28,32].

3.3. Antibacterial spectrum and MIC of velezin

The antibacterial spectrum of velezin was shown in Table 1. The velezin demonstrated excellent antibacterial activity against Gram-positive including *Enterococcus*, *Staphylococcus* and *Bacillus*. This result was consistent with the typical features of bacteriocins, which usually present the narrow inhibitory activities against closely related species to the producers [5]. Velezin showed decent activity against *L. monocytogenes* ATCC 19115 with a MIC as low as 2 μg/mL, higher than that of circular bacteriocins enterocin AS-48 (as reported at 0.1 μg/mL) [16]. It was of note that velezin also exhibited antibacterial activities against some Gram-negative bacteria including, *Escherichia*, *Cronobacter* and *Acinetobacter*, which is seldom documented with circular bacteriocins including enterocin

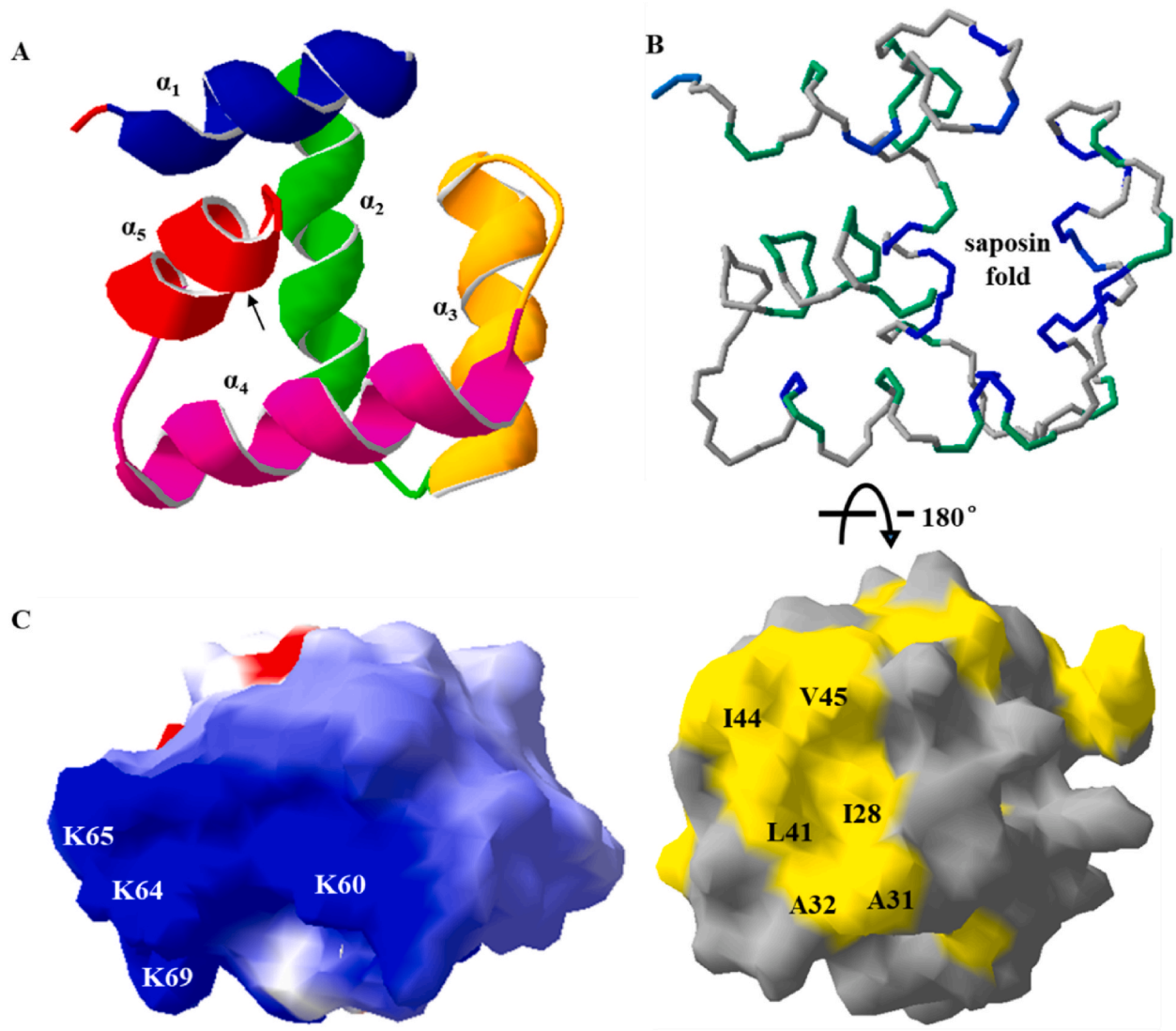

Fig. 4. Structural predication of velezin by AlphaFold2. (A) Ribbon diagram of velezin. Helices α_1, α_2, α_3, α_4 and α_5 are colored in blue, green, orange, and red, respectively, with a black arrow indicating the position of the N-to-C cyclization. (B) Hydrophobic structure of velezin: up: backbone hydrophobic core of saposin fold, with hydrophobicity from Ile, Leu, Val, and Phe marked in dark blue whereas hydrophobicity from Ala and Met marked in light blue; down, surface plot illustrating solvent exposed hydrophobic residues (yellow). (C) Electrostatic surface potential of velezin, with blue and red indicating positive and negative charge, respectively.

AS-48. This was possibly due to that the three aforementioned Gram-negative strains might be co-inhabited in the ecological niche together with *B. velezensis* 1-3 [5]. Taken together, the results of this study indicated that velezin had an antibacterial spectrum broader than other circular bacteriocins have been reported.

Interestingly, velezin also demonstrated inhibitory ability against fungi such as *C. albicans*, *R. solani*, and *A. versicolor* (Table 1), which is rarely documented in circular bacteriocin [11].

3.4. The hemolysis and cytotoxicity assay

Hemolysis degree is a common measure used for safety assessment. The hemolytic potential of velezin was determined by the percentage of lysed red cells using mouse erythrocytes. It was found that velezin did not cause apparent hemolytic effect (usually taken as positive when the rate of hemolysis is >5 %) at and below 2 × MIC. However, velezin may lead to hemolysis at concentrations beyond 4 × MIC (Fig. 5A). Similar hemolytic effect results have been observed with circular bacteriocin enterocin NKR-5-3B when human red blood cells was tested [29].

If formulated or included in a food or feed additive, the direct contact of circular bacteriocin to intestinal epithelial cells might

Table 2
Characterization of gene cluster of velezin.

Cluster No.[a]	Position in the genome	Transcriptome sequence No.	TPM	Homology[b]	Putative function
orf00003	LLZC01000018[+] 311218-313194	AR442_06870	6.08	P39839 (*Bacillus subtilis*), 68.2 %	Uncharacterized peptidase YuxL (Charge relay system)
orf00007	LLZC01000018[+] 313650-313976	AR442_06880	16.55	O32118 (*B. subtilis*), 76.9 %	disulfide oxidoreductase YuzD
orf00010	LLZC01000018[+] 315348-315584	AR442_06890	3.67	A7Z8D5 (*B. velezensis*), 100 %	UPF0349 protein
orf00013	LLZC01000018[+] 315719-316936	AR442_06895	0.28	O32115 (*B. subtilis*), 91.1 %	Uncharacterized transporter YutK
orf00015	LLZC01000018[+] 317060-317914	AR442_06900	19.53	A7Z8D3 (*B. velezensis*), 100 %	Diaminopimelate epimerase
orf00017	LLZC01000018[+] 317991-318353	AR442_06905	14.72	O32113 (*B. subtilis*), 90 %	Uncharacterized protein SufA
orf00024	LLZC01000018[+] 321327-321899	AR442_06930	3.61	G2TKA9 (*Weizmannia coagulans*)	Yip1 domain-containing protein (integral component of membrane)
orf00025	LLZC01000018[+] 321967-322302	AR442_06935	348.85	V9WBZ6 (*Paenibacillus larvae*), 78.9 %	Putative circular bacteriocin velezin
orf00030	LLZC01000018[+] 322385-324040	AR442_06940	2.66	V9WCD2 (*P. larvae*), 52 %	ABC-2 type transport system permease protein (integral component of membrane)
orf00031	LLZC01000018[+] 324033-324737	AR442_06945	3.6	V9W8M0 (*P. larvae*), 73.5 %	ABC transporter ATP-binding protein
orf00034	LLZC01000018[+] 324734-325261	AR442_06950	3.54	V9WE48 (*P. larvae*), 53.7 %	stage II sporulation protein M (integral component of membrane)
orf00035	LLZC01000018[+] 325278-325499	AR442_06955	0.9	V9WB28(*P. larvae*), 61.2 %	CPBP family intramembrane metalloprotease
orf00044	LLZC01000018[+] 328247-329467	AR442_06970	46.61	O05267 (*B. subtilis*), 89.4 %	NADH dehydrogenase-like protein YumB
orf00048	LLZC01000018[+] 329830-330156	AR442_06975	242.85	O32109 (*B. subtilis*), 83 %	Uncharacterized membrane protein YuiB (integral component of membrane)
orf00050	LLZC01000018[+] 330281-330898	AR442_06980	28.53	O32109 (*B. subtilis*), 72.1 %	Uncharacterized protein YuiC (outer membrane)

[a] Velezin gnen cluster prediction in *B. velezensis* strain NRRL B-41580 genomic sequence by the BAGEL4 online program.
[b] Homology (percentage of identical amino acid sequence) to genes present in the other genes sequences with GenBank accession numbers.

rouses concerns such as potential cytotoxicity or other possible damages to the intestine [11,13]. *In vitro* cytotoxicity tests via resazurin assay were conducted with Caco-2 cell line using velezin at concentrations ranging from 2 to 256 μg/mL (1-128 × MIC) respectively. As shown in Fig. 5B, velezin did not show any cytotoxicity to Caco-2 cells, even at the concentration up to 128 μg/mL (Caco-2 cells still remained 97.8 % viability). Cebrián et al. have ever showed that the circular bacteriocin enterocin AS-48 had hemolysis to defibrinated erythrocytes (the percent hemolysis was 3%–22.6 %) at the concentration of 5–20 μmol/L, but had no cytotoxicity to MCF10A and CCDC18Co human cells at higher concentrations ranging from 0.27 to 27 μmol/L [33]. Thus far, bacteriocins, including nisin, the first one entitled with Generally Recognized as Safe status [9], are generally considered as safe for food or feed use. Facilitated with its cytotoxicity-free nature, it is reasonable to assume that velezin might find its applications as a safe additive used in food or feed in the future.

3.5. Stability of velezin

As aforementioned, through structure-activity potency analysis, we assumed that velezin would be stable against adverse conditions met in food processing. To verify this, a panel tests applied to challenge velezin with a series of temperature, pH variation and proteolytic enzymes treatments (Fig. 5C–E). It was found that the antibacterial activity of velezin was not altered when it was exposed to temperatures ranging from 20 °C to 100 °C for 10 min (Fig. 5C). Velezin remained stable under neutral and alkaline (pH, 6.0–10.0) conditions, but its activity was reduced when it challenged by acidic conditions (pH, 2.0–4.0) (Fig. 5D). It was well documented for other circular bacteriocins that the cross-linkage of the termini decreases the conformational entropy of the disordered and highly flexible linear polypeptides, and thus renders the stability of the circular bacteriocins [33]. The above stability features of velezin might be also attributed by its circular covalent bond formed within the molecule. In this study, it was observed that velezin retained its antimicrobial activity even when it was treated with a panel of proteases, including trypsin, papain, chymotrypsin, pepsin and protease K, respectively (Fig. 5E). Similar features have been found with other circular bacteriocins such as plantaricyclin A [24], lactocyclicin Q [34] and leucocyclicin Q [35]. The circular structures are considered to reduce the availability of possible cleavage sites and thus provide the circular bacteriocins with resistance to protease hydrolysis [11].

3.6. Inhibitory effect against biofilm formation

The ability of biofilm formation of *L. monocytogenes* makes it a major challenge for the food industry, since the biofilms endows the

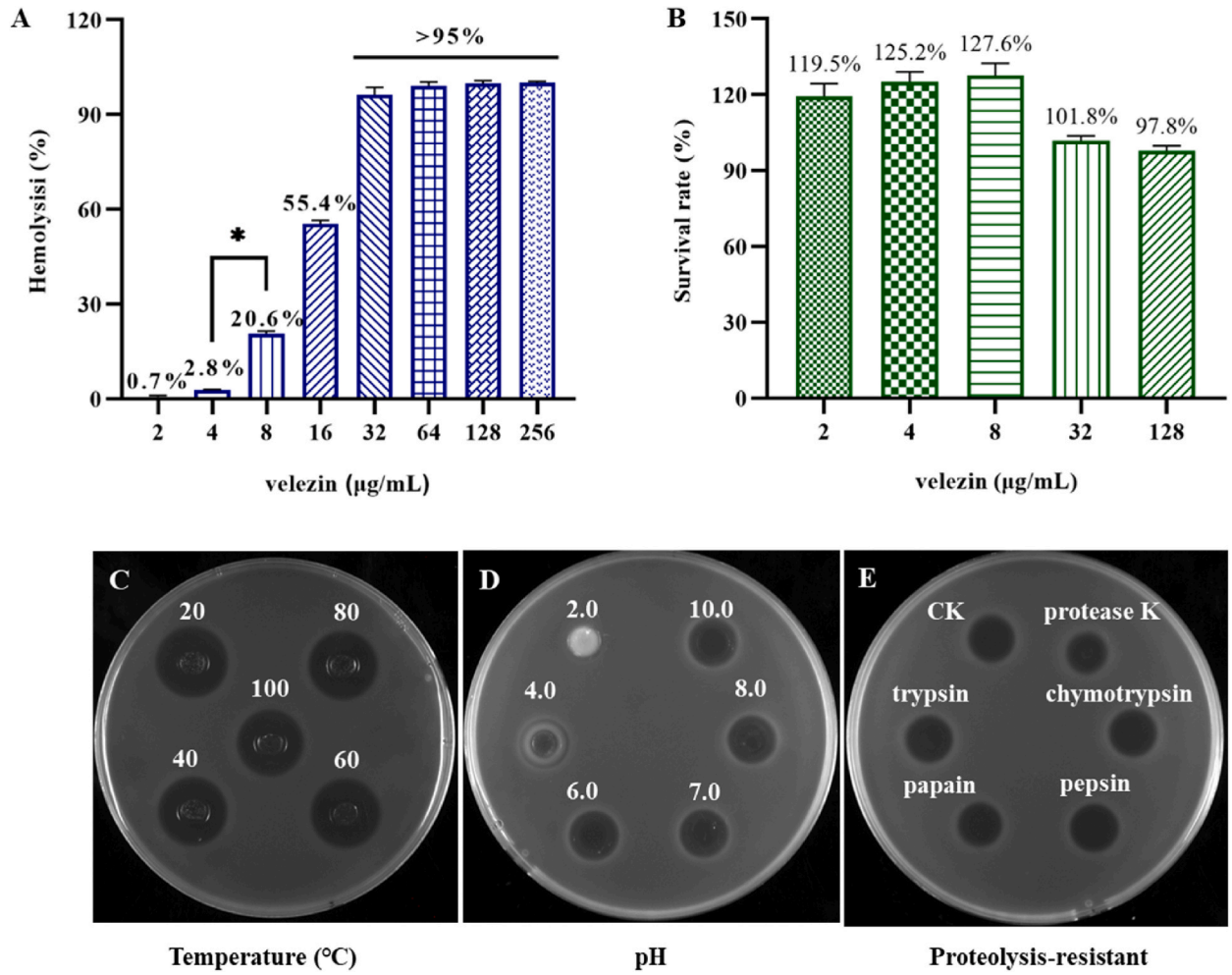

Fig. 5. Toxicity, stability and proteolysis-resistant of velezin. (A) Hemolytic activity of velezin against fresh mouse erythrocyte. (B) Cytotoxicity of the peptides against Caco-2 cells. Results are presented as mean ± SD (n = 3). *$p < 0.05$. (C)–(E) Effects of temperature, pH, and proteases on the antibacterial activity of velezin against *L. monocytogenes*, respectively.

persistence of the bugs on the surfaces of food processing equipment and facilities [3]. Chemical substances such as sodium lactate, sodium hypochlorite, and hydrogen peroxide have been recognized as effective for the control of biofilms [36]. However, some well-known drawbacks of these measures have arisen concerns over the chemical residues [36]. Due to the natural safety features, bacteriocins have been drawing considerable attentions regarding their potential use in inhibiting biofilm formation [36–38]. In this work, it was confirmed that velezin demonstrated promising potential in inhibiting *L. monocytogenes* from biofilm formation (Fig. 6A). Velezin could effectively inhibit the biofilm formation of *L. monocytogenes* at 2 μg/mL (inhibition rate 44.95 %), and when its concentration getting higher (4 and 8 μg/mL), velezin did demonstrate equal or even better biofilm inhibition effects compared to that of sodium lactate (at 5 %), the recommended solution to inhibit the growth of *L. monocytogenes* in ready-to-eat foods permitted by the U.S. Department of Agriculture–Food Safety and Inspection Service (50.31 % and 58.66 % of velezin versus 54.36 % of 5 % sodium lactate, $p > 0.05$) [39]. The above results indicated that velezin may have decent potential to be further explored on the inhibition of the biofilm formation by *L. monocytogenes*.

3.7. Inhibition pattern of velezin

A growth inhibition assay was used to investigate the antimicrobial pattern of velezin against *L. monocytogenes* ATCC 19115. As showed in Fig. 6B, compared to untreated group, the exposure to 1 × -4 × MIC of velezin for 4 h reduced the viable indicator cell counts by 0.94–1.27 in log CFU/mL. When the exposure time with 1 × and 2 × MIC of velezin was extended to 8 and 12 h, the viable indicator cell counts dropped approximately by 1.3 and 2.3 in log CFU/mL, respectively. The most evident inhibitory effect was observed with velezin at 4 × MIC, with a reduction of the indicators amounting to 3.5 in log CFU/mL after the treatment of 12 h. The significant differences analyses among all treatments was shown in Fig. 6b, the results indicated that the inhibitory effect of velezin against

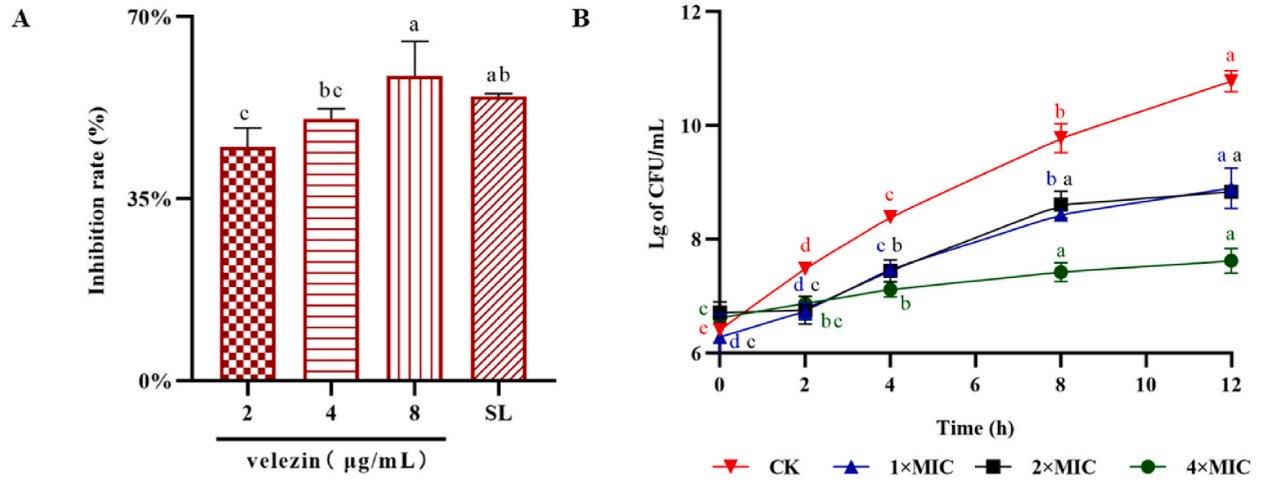

Fig. 6. Activity of velezin against *L. monocytogenes*. The inhibition rate of biofilm formation (A) and viable count (B) of *L. monocytogenes* in the presence of velezin at 2, 4 and 8 μg/mL were showed. Results were presented as mean ± SD (n = 3). Different lowercase letters indicated the significant differences ($p < 0.05$).

L. monocytogenes fell into a concentration-dependent yet time-related pattern, whereas with the treatment of velezin the rebounding growth of the indicator bugs were largely retarded by at least 4 h ($p < 0.05$). The above result might indicate that velezin perform a bacteriostatic mode of action, differed from the bactericidal mode that had been found in some other circular bacteriocins [38–42].

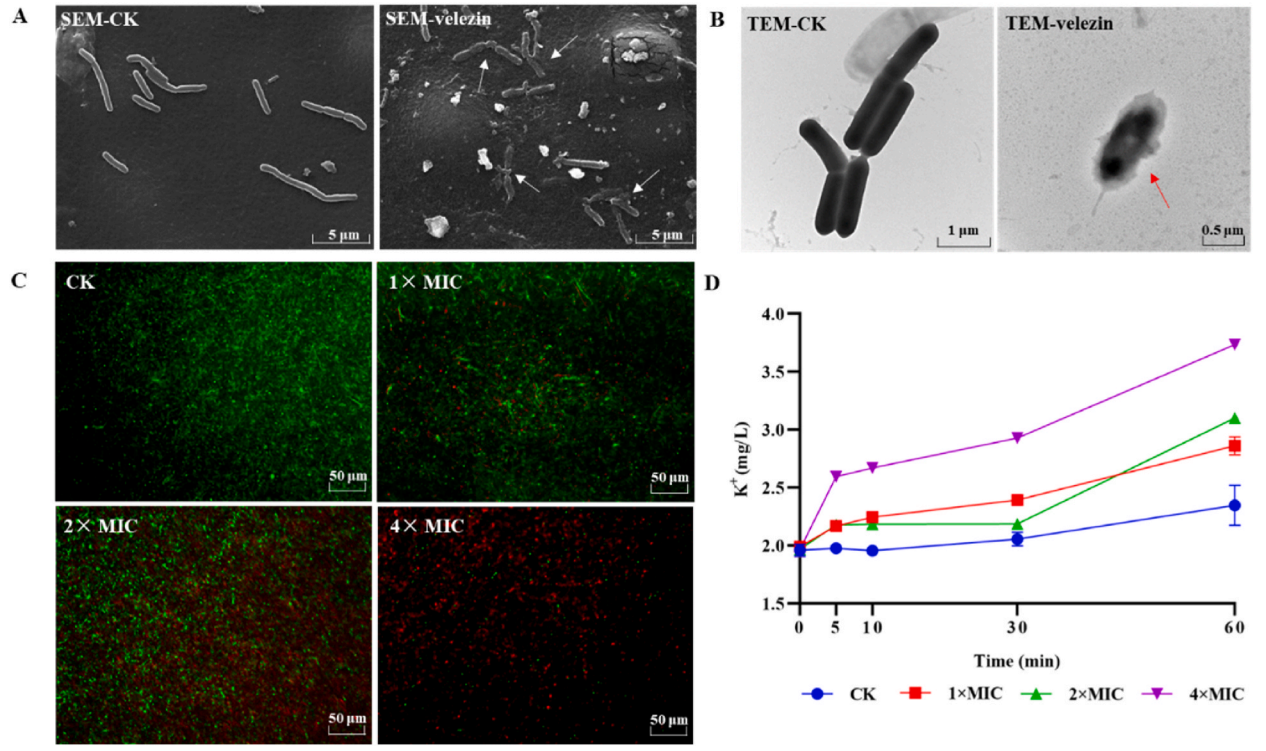

Fig. 7. Mode of action of velezin against *L. monocytogenes*. (A) Cells were treated with 4 × MIC velezin, SEM observation: it was identified that the shrinked and wrinkled cells were identified in treatment group, but the full shape and smooth surface cells were identified in control group. (B) Cells were treated with 4 × MIC velezin, TEM observation: the regular rod-shaped and homogeneous electron density of the cells were identified in control group, but unclear boundary of the cells were identified in treatment group. (C) Cells were treated with 1 × to 4 × MIC velezin, inverted fluorescence microscope observation: live cells were stained in green by AO and dead cells were stained in red from PI. With the increase of bacteriocin concentration, the number of dead cells (red) gradually increased, while the number of live cells (green) gradually decreased. (D) Determination of potassium ions after the treatment of velezin: CK, the untreated *L. monocytogenes* cells. Results were presented as mean ± SD (n = 3).

3.8. SEM and TEM analyses

The impact of velezin on the morphology of indicator strains was investigated by using SEM. The untreated cells of *L. monocytogenes* appeared as plump cells rod in shape with smooth surface. In contrast, the velezin treated *L. monocytogenes* cells became shrinked and wrinkled (Fig. 7A). TEM images of *L. monocytogenes* showed regular rod-shaped intact cells with homogeneous electron density in control treatment, whereas the velezin treated cells became damaged showing unclear boundaries as well as exhibiting unevenly-distributed electron density (Fig. 7B). Similar morphological alterations were also observed for *Propionibacterium acnes* that was treated with enterocin AS-48 [43] and *S. aureus* that was treated with enterocin OE-12 [41]. In conclusion, the SEM and TEM observations revealed that velezin exerted its antibacterial activity through alterations of the cell membrane or of cell wall of target cells.

3.9. Effect of velezin on the viability of L. monocytogenes

In order to further confirm the destructive effect of velezin on the cell membrane of *L. monocytogenes*, a PI/AO co-staining assay was applied, in which cells with the impaired membrane can only be stained with PI, while the viable cells are stained by AO [44]. The cells in negative control were stained green, indicating cells with intact cell membrane only taking AO but not PI (Fig. 7C). With velezin treated at varied concentrations, the incessant accumulation of PI uptake was observed along with the increase of velezin concentration; in contrast, the AO uptake displayed an opposite trend, and a declined reddish pattern was sighted (Fig. 7C). Taken together, the staining assay results also revealed that velezin could disrupt the membrane integrity of *L. monocytogenes*.

3.10. Membrane permeability detection

Membrane permeability tests was conducted via measuring the efflux of potassium ions by applying a classical method used for other bacteriocins for the same purpose [23]. The intracellular K^+ concentration of negative control remained stable within 60 min (Fig. 7D). However, once treated with 1 × , 2 × and 4 × MIC velezin for 5 min, the indicator cells lost 11.4 %, 12.3 % and 33.7 % of intracellular K^+ (reflected by the K^+ concentration in the supernatant), respectively (Fig. 7D). When treatment time extending to 60 min, the K^+ concentration in the supernatant increased apparently up to 34.9 %, 46.2 % and 75.9 %, respectively. Similar effects were also observed in other circular bacteriocins like gassericin A [45], carnocyclin A [46] and enterocin AS-48 [16]. In this study, additional tests were attempted to examine the release of intracellular proteins and DNA. However, no significant differences between the experimental group and the control group the extracellular were detected (data not show). This might be due to that the velezin induced pores in the membranes of target cells were neither too narrow nor improperly oriented for the two big molecules to transport out transmembrane-wise via overcoming other resistance such as hydrophobic interaction.

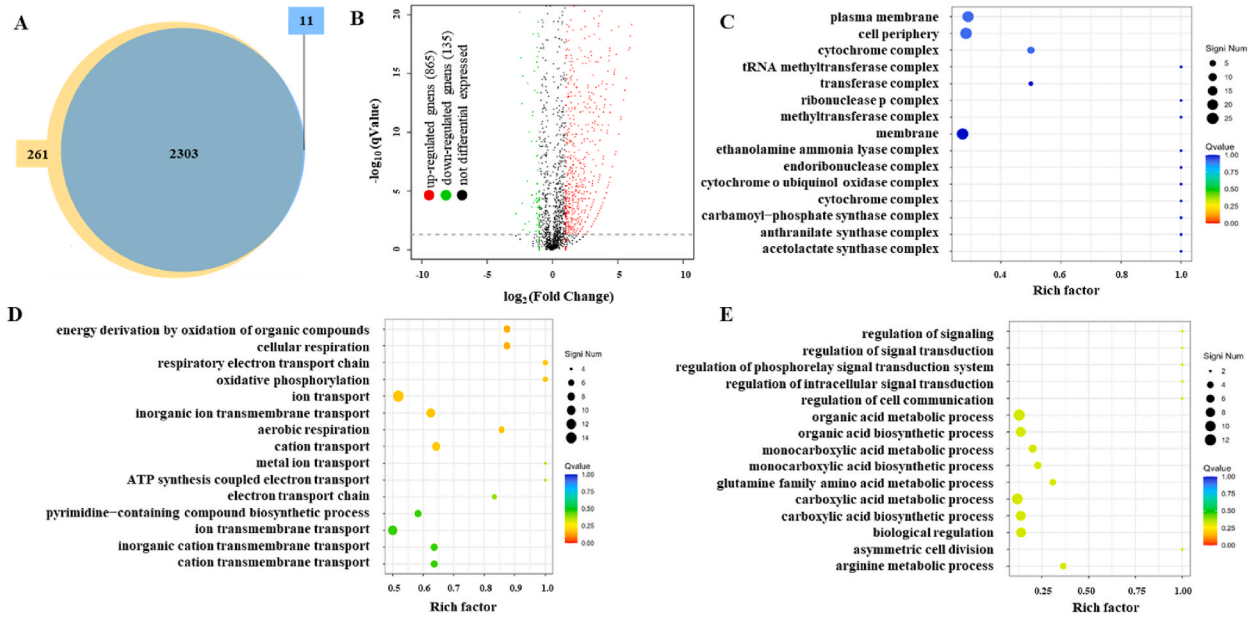

Fig. 8. Transcriptional response of *L. monocytogenes* at the challenge of velezin at 0.5 × MIC. (A) Venn diagram showing 261 and 11 genes was independently expressed in the treatment (orange) and control (light blue) group, 2303 genes were shared by both groups (dark blue). (B) Volcano diagram showing that among the differential genes, 865 were up-regulated (red) and 135 were down-regulated (green). (C) GO analysis of genes up-regulated in *L. monocytogenes* for CC. (D) GO analysis of genes up-regulated in *L. monocytogenes* for BP. (E) GO analysis of genes down-regulated in *L. monocytogenes* for BP, with the top 15 enrichment pathways shown in the scatter plot; size of the bubble represented the number of genes enriched in the GO terms, and color showed the q-value of GO terms.

3.11. Effect of velezin on gene expression in *L. monocytogenes*

To determine the transcriptional response of *L. monocytogenes* ATCC19115 at the challenge of velezin, a sub-inhibitory concentration of the bacteriocin (1 μg/mL) was applied. Through RNA sequencing, 2, 575 genes were identified from the two datasets. Of them, some genes were specific for the treatment (261 out of 2, 575) and the control group (11 out of 2, 575), respectively, while others were shared by both groups (2, 303 out of 2, 575) (Fig. 8A). To screen the differentially expressed genes between the treatment and the control group, the absolute value of $\log_2$ fold change ≥ 1 and q value ≤ 0.05 was taken as the threshold. The results showed that totally 991 of the *L. monocytogenes* genes were altered at transcription level. Among them, 856 were up-regulated while 135 were down-regulated when compared to the control group (Fig. 8B). The distribution of the differentially expressed genes was studied by GO enrichment analysis for gene function in terms of cellular component (CC), molecular function (MF), and biological process (BP). The results showed that the genes expressed were involved in 771 terms for BP, 365 terms for MF and 56 terms for CC, respectively. The most enriched GO terms were related to small molecule metabolic process, ion transport, and plasma membrane. Of them, the significantly down-regulated genes were mostly involved in organic acid biosynthetic and metabolic, whereas the up-regulated genes generally encoded ion transport, cell wall macromolecule biosynthetic and metabolic process, and pyrimidine and ATP biosynthetic process (Supplementary Fig. S5).

In CC terms, the up-regulated genes encoded membrane-associated proteins (Fig. 8C), while the down-regulated genes were related with intracellular part and cytoplasm. Like most other bacteriocins, when applied velezin could disrupt the membrane of the indicator cells. It is possible that the observed overexpression of membrane-associated genes is just an immediate response of the bugs to the challenge of velezin, and furtherly a successive compensation or repairing attempts for the dysfunction of the membrane. Grande Burgos et al. also reported that the genes encode membrane-associated were up-regulated in *Bacillus cereus* ATCC 14579 after treated with enterocin AS-48 at subinhibitory concentration [47].

In MF terms, the up-regulated genes encoded transferase, ion transmembrane transporter and catalytic activity, whereas the down-regulated genes encoded small molecule and nucleotide binding proteins (Supplementary Fig. S6). Up-regulation of ion transporter gene expression might be used to compensate for potassium ion leakage caused by velezin.

In BP terms, some genes for encoding ion transport and carbohydrate derivative biosynthetic process were up-regulated (Fig. 8D), while organic acid metabolic and biosynthetic process were down-regulated (Fig. 8E). The reduction of organic acid somehow may reduce the binding tendency of velezin to the cell surface of *L. monocytogenes* ATCC19115, just as documented with the case of *B. cereus* at the change of enterocin AS-48 [47].

As aforementioned velezin inhibited biofilm formation by *L. monocytogenes* ATCC19115. However, the differential expression of biofilm-related genes was not observed at the presence of velezin. This might be due to that a response time merely 5 h may be too short for the indicator to manage the population level coordination and or communication regarding the simultaneously initiating the group of related genes functionate consonantly. It has been reported that the expression of *L. monocytogenes* biofilm-related genes was significantly different after 24 h of treatment with olive leaf extract, but the differentially expressed genes were not found in 3.5 h of treatment [48]. Similarly, after 16 h of treatment with sublethal doses of bacteriocins lactocin AL705, there was a significant abundance increase with protein related to biofilm synthesis by *L. monocytogenes* [49].

In addition, at the challenge of nisin, a unique cold shock proteins (Csps), well-recognized indicator for stress responses by this bug, was significantly up-regulated by *L. monocytogenes* [2,9]. In this study, the transcriptome analysis results did showed that the transcript abundances of *cspB* and *cspD* were significantly upregulated (increase from 1221.97 to 2667.66 and from 105.54 to 499.68, respectively) when *L. monocytogenes* was challenged with 0.5 × MIC velezin.

4. Conclusion

According to the best of our knowledge, this is the first report on the characterization of a circular bacteriocin velezin by *B. velezensis*. It demonstrated a broad antimicrobial spectrum against a panel of microorganisms, including Gram-positives, a few Gram-negative as well as a few fungi pathogens. The MIC of velezin against *L. monocytogenes* ATCC 19115 was as low as 2 μg/mL. Velezin exerted its bacteriostatic effect against *L. monocytogenes* ATCC 19115 by increasing membrane permeability and damaging the integrity of membrane. Velezin could retain its activity under varied temperatures and pH conditions. It was noteworthy that velezin was resistant to the hydrolysis of a panel of proteases tested. Moreover, velezin presented no cytotoxicity to Caco-2 cells. Taken together, velezin might have potential to be used for food/feed in the future. It was noteworthy that at the challenge by sub-inhibitory doses of velezin, a panel of genes that involved in membrane proteins, ion transporters, proteins for small molecule synthesis and cold shock proteins, were up-regulated by *L. monocytogenes* ATCC 19115. This finding may provide useful clues for research in the future, particularly in the solution-seeking to the possible defensive response of *L. monocytogenes* when it challenged with circular bacteriocins.

Data availability statement

The strain, *B. velezensis* 1–3, has been collected at the CGMCC (https://cgmcc.net/) under the Accession number is CGMCC No. 25292. Data associated with this study has been deposited at the NMDC (https://nmdc.cn/) under the Accession number of *B. velezensis* 16S rDNA gene is NMDCN0000QQ7.

CRediT authorship contribution statement

Jun Zhang: Writing – original draft, Project administration, Methodology. **Lihong Zhao:** Project administration, Methodology. **Wei Tang:** Resources, Project administration, Conceptualization. **Jiaxin Li:** Methodology, Investigation. **Tao Tang:** Methodology, Investigation. **Xiaowen Sun:** Methodology, Investigation. **Xiaoni Qiao:** Methodology, Investigation. **Zengguo He:** Writing – original draft, Resources, Investigation, Data curation, Conceptualization.

Declaration of competing interest

The authors declare that they have no known competing financial interests or personal relationships that could have appeared to influence the work reported in this paper.

Acknowledgments

This work was supported by the Science and Technology Projects in Key areas of Guangdong [grant number 2020B0202010001]; and the TaiShan industrial Experts Programme [grant number tscy202006017].

Appendix A. Supplementary data

Supplementary data to this article can be found online at https://doi.org/10.1016/j.heliyon.2024.e29701.

References

[1] World Health Organizatio, Listeriosis, World Health Organization, Geneva, Switzerland, 2018. https://www.who.int/news-room/fact-sheets/detail/listeriosis.
[2] F. Muchaamba, R. Stephan, T. Tasara, *Listeria monocytogenes* cold shock proteins: small proteins with a huge impact, Microorganisms 9 (5) (2021) 1061, https://doi.org/10.3390/microorganisms9051061.
[3] L.T. Matereke, A.I. Okoh, *Listeria monocytogenes* virulence, antimicrobial resistance and environmental persistence: a review, Pathogens 9 (7) (2020) 528, https://doi.org/10.3390/pathogens9070528.
[4] J. Wu, O. McAuliffe, C.P. O'Byrne, Manganese uptake mediated by the NRAMP-type transporter MntH is required for acid tolerance in *Listeria monocytogenes*, Int. J. Food Microbiol. 399 (2023) 110238, https://doi.org/10.1016/j.ijfoodmicro.2023.110238. Epub 2023 May 2.
[5] J. Zhang, Q. Wang, W. Tang, G. Liu, X. Xu, Z. He, Bacteriocinogeny, the way to acquire survival advantages through biosynthetic regulation: a review, Microbiol. China 47 (3) (2020) 923–932, https://doi.org/10.13344/j.microbiol.china.190617.
[6] J. Vaca, A. Ortiz, E. Sansinenea, *Bacillus* sp. bacteriocins: ntural weapons against bacterial enemies, Curr. Med. Chem. 29 (12) (2022) 2093–2108, https://doi.org/10.2174/0929867328666210527093041.
[7] E.M. Johnson, Y.G. Jung, Y.Y. Jin, R. Jayabalan, S.H. Yang, J.W. Suh, Bacteriocins as food preservatives: challenges and emerging horizons, Crit. Rev. Food Sci. Nutr. 58 (16) (2018) 2743–2767, https://doi.org/10.1080/10408398.2017.1340870.
[8] J. Vaca, A. Ortiz, E. Sansinenea, A study of bacteriocin like substances comparison produced by different species of *Bacillus* related to *B. cereus* group with specific antibacterial activity against foodborne pathogens, Arch. Microbiol. 205 (1) (2022) 13, https://doi.org/10.1007/s00203-022-03356-0.
[9] F. Muchaamba, J. Wambui, R. Stephan, T. Tasara, Cold shock proteins promote nisin tolerance in *Listeria monocytogenes* through modulation of cell envelope modification responses, Front. Microbiol. 12 (2021) 811939, https://doi.org/10.3389/fmicb.2021.811939 eCollection 2021.
[10] B. Xin, H. Liu, J. Zheng, C. Xie, Y. Gao, D. Dai, D. Peng, L. Ruan, H. Chen, M. Sun, *In silico* analysis highlights the diversity and novelty of circular bacteriocins in sequenced microbial genomes, mSystems 5 (3) (2020) e00047, https://doi.org/10.1128/mSystems.00047-20, 20.
[11] C. Gabrielsen, D.A. Brede, I.F. Nes, D.B. Diep, Circular bacteriocins: biosynthesis and mode of action, Appl. Environ. Microbiol. 80 (22) (2014) 6854–6862, https://doi.org/10.1128/AEM.02284-14. Epub 2014 Aug 29.
[12] Y. Masuda, T. Zendo, K. Sonomoto, New type non-lantibiotic bacteriocins: circular and leaderless bacteriocins, Benef. Microbes 3 (1) (2012) 3–12, https://doi.org/10.3920/BM2011.0047.
[13] R.H. Perez, T. Zendo, K. Sonomoto, Circular and leaderless bacteriocins: biosynthesis, mode of action, applications, and prospects, Front. Microbiol. 9 (2018) 2085, https://doi.org/10.3389/fmicb.2018.02085.eCollection2018.
[14] M. Maqueda, M. Sánchez-Hidalgo, M. Fernández, M. Montalbán-López, E. Valdivia, M. Martínez-Bueno, Genetic features of circular bacteriocins produced by Gram-positive bacteria, FEMS Microbiol. Rev. 32 (1) (2008) 2–22, https://doi.org/10.1111/j.1574-6976.2007.00087.x. Epub 2007 Nov 20.
[15] J. Zhang, W. Tang, X. Sun, X. Liu, Z. He, Research progress of circular bacteriocin, Acta. Microbiol. Sinica. 62 (7) (2022) 2498–2508, https://doi.org/10.13343/j.cnki.wsxb.20210714.
[16] M.J. Grande Burgos, R.P. Pulido, M. Del Carmen López Aguayo, A. Gálvez, R. Lucas, The cyclic antibacterial peptide enterocin AS-48: isolation, mode of action, and possible food applications, Int. J. Mol. Sci. 15 (12) (2014) 22706–22727, https://doi.org/10.3390/ijms151222706.
[17] J. Zhang, L. Zhang, W. Tang, X. Sun, T. Tang, X. Qiao, M. Liang, Z. He, Purification, identification, and characterization of surfactin from *Bacillus velezensis* 1-3, Food Sci. (N. Y.) 44 (4) (2023) 177–184, https://doi.org/10.7506/spkx1002-6630-20220326-326.
[18] J. Zhang, Y.Y. Yang, D. Teng, Z. Tian, S. Wang, J. Wang, Expression of plectasin in *Pichia pastoris* and its characterization as a new antimicrobial peptide against *Staphyloccocus* and *Streptococcus*, Protein Expr. Purif. 78 (2) (2011) 189–196, https://doi.org/10.1016/j.pep.2011.04.014. Epub 2011 May 4.
[19] Z. He, D. Kisla, L. Zhang, C. Yuan, K.B. Green-Church, A.E. Yousef, Isolation and identification of a *Paenibacillus polymyxa* strain that coproduces a novel lantibiotic and polymyxin, Appl. Environ. Microbiol. 73 (1) (2007) 168–178, https://doi.org/10.1128/AEM.02023-06. Epub 2006 Oct 27.
[20] L.H. Zhao, X.P. Lin, J.Y. Fu, J. Zhang, W. Tang, Z. He, A novel bi-functional fibrinolytic enzyme with anticoagulant and thrombolytic activities from a marine-derived fungus *Aspergillus versicolor* ZLH-1, Mar. Drugs 20 (6) (2022) 356, https://doi.org/10.3390/md20060356.
[21] N. Yang, D. Teng, R. Mao, Y. Hao, X. Wang, Z. Wang, X. Wang, J. Wang, A recombinant fungal defensin-like peptide-P2 combats multidrug-resistant *Staphylococcus aureus* and biofilms, Appl. Microbiol. Biotechnol. 103 (13) (2019) 5193–5213, https://doi.org/10.1007/s00253-019-09785-0. Epub 2019 Apr 25.
[22] Q. Zhang, N. Yang, R. Mao, Y. Hao, X. Ma, D. Teng, H. Fan, J. Wang, A recombinant fungal defensin-like peptide-P2 combats *Streptococcus dysgalactiae* and biofilms, Appl. Microbiol. Biotechnol. 105 (4) (2021) 1489–1504, https://doi.org/10.1007/s00253-021-11135-y. Epub 2021 Feb 3.
[23] H. Du, J. Yang, X. Lu, Z. Lu, X. Bie, H. Zhao, C. Zhang, F. Lu, Purification, characterization, and mode of action of plantaricin GZ1-27, a novel bacteriocin against *Bacillus cereus*, J. Agric. Food Chem. 66 (18) (2018) 4716–4724, https://doi.org/10.1021/acs.jafc.8b01124. Epub 2018 May 1.

[24] J. Borrero, E. Kelly, P.M. O'Connor, P. Kelleher, C. Scully, P.D. Cotter, J. Mahony, D. van Sinderen, A. Plantaricyclin, A novel circular bacteriocin produced by *Lactobacillus plantarum* NI326: purification, characterization, and heterologous production, Appl. Environ. Microbiol. 84 (1) (2017) e01801, https://doi.org/10.1128/AEM.01801-17, 17.
[25] J.Z. Acedo, M.J. van Belkum, C.T. Lohans, R.T. McKay, M. Miskolzie, J.C. Vederas, Solution structure of acidocin B, a circular bacteriocin produced by *Lactobacillus acidophilus* M46, Appl. Environ. Microbiol. 81 (8) (2015) 2910–2918, https://doi.org/10.1128/AEM.04265-14. Epub 2015 Feb 13.
[26] L.A. Martin-Visscher, X. Gong, M. Duszyk, J.C. Vederas, The three-dimensional structure of carnocyclin A reveals that many circular bacteriocins share a common structural motif, J. Biol. Chem. 284 (42) (2009) 28674–28681, https://doi.org/10.1074/jbc.M109.036459. Epub 2009 Aug 18.
[27] R. Cebrian, M. Martinez-Bueno, E. Valdivia, A. Albert, M. Maqueda, M.J. Sánchez-Barrena, The bacteriocin AS-48 requires dimer dissociation followed by hydrophobic interactions with the membrane for antibacterial activity, J. Struct. Biol. 190 (2) (2015) 162–172, https://doi.org/10.1016/j.jsb.2015.03.006. Epub 2015 Mar 27.
[28] C. Gabrielsen, D.A. Brede, Z. Salehian, I.F. Nes, D.B. Diep, Functional genetic analysis of the GarML gene cluster in *Lactococcus garvieae* DCC43 gives new insights into circular bacteriocin biosynthesis, J. Bacteriol. 196 (5) (2014) 911–999, https://doi.org/10.1128/JB.01115-13. Epub 2013 Dec 13.
[29] K. Himeno, K.J. Rosengren, T. Inoue, R.H. Perez, M.L. Colgrave, H.S. Lee, L.Y. Chan, S.T. Henriques, K. Fujita, N. Ishibashi, Identification, characterization, and three-dimensional structure of the novel circular bacteriocin, enterocin NKR-5-3B, from *Enterococcus faecium*, Biochemistry 54 (31) (2015) 4863–4876, https://doi.org/10.1021/acs.biochem.5b00196. Epub 2015 Jul 31.
[30] A. Toplak, T. Nuijens, P.J. Quaedflieg, B. Wu, D.B. Janssen, Peptiligase, an enzyme for efficient chemoenzymatic peptide synthesis and cyclization in water, Adv. Synth. Catal. 358 (2016) 2140–2147, https://doi.org/10.1002/adsc.201600017.
[31] K.B. Narayanan, S.S. Han, Peptide ligases: a novel and potential enzyme toolbox for catalytic cross-linking of protein/peptide-based biomaterial scaffolds for tissue engineering, Enzyme. Microb. Technol. 155 (2022) 109990, https://doi.org/10.1016/j.enzmictec.2022.109990. Epub 2022 Jan 7.
[32] R. Kemperman, M. Jonker, A. Nauta, O.P. Kuipers, J. Kok, Functional analysis of the gene cluster involved in production of the bacteriocin circularin A by *Clostridium beijerinckii* ATCC 25752, Appl. Environ. Microbiol. 69 (10) (2003) 5839–5848, https://doi.org/10.1128/AEM.69.10.5839-5848.2003.
[33] R. Cebrián, M.E. Rodríguez-Cabezas, R. Martín-Escolano, S. Rubiño, M. Garrido-Barros, M. Montalbán-López, M.J. Rosales, M. Sánchez-Moreno, E. Valdivia, M. Martínez-Bueno, Preclinical studies of toxicity and safety of the AS-48 bacteriocin, J. Adv. Res. 20 (2019) 129–139, https://doi.org/10.1016/j.jare.2019.06.003.eCollection2019Nov.
[34] N. Sawa, T. Zendo, J. Kiyofuji, K. Fujita, K. Himeno, J. Nakayama, K. Sonomoto, Identification and characterization of lactocyclicin Q, a novel cyclic bacteriocin produced by *Lactococcus* sp. strain QU 12, Appl. Environ. Microbiol. 75 (6) (2009) 1552–1558, https://doi.org/10.1128/AEM.02299-08. Epub 2009 Jan 9.
[35] Y. Masuda, H. Ono, H. Kitagawa, H. Ito, F. Mu, N. Sawa, T. Zendo, K. Sonomoto, Identification and characterization of leucocyclicin Q, a novel cyclic bacteriocin produced by *Leuconostoc mesenteroides* TK41401, Appl. Environ. Microbiol. 77 (22) (2011) 8164–8170, https://doi.org/10.1128/AEM.06348-11. Epub 2011 Sep. 23.
[36] A.C. Camargo, S.D. Todorov, N.E. Chihib, D. Drider, L.A. Nero, Lactic acid bacteria (LAB) and their bacteriocins as alternative biotechnological tools to control *Listeria monocytogenes* biofilms in food processing facilities, Mol. Biotechnol. 60 (9) (2018) 712–726, https://doi.org/10.1007/s12033-018-0108-1.
[37] H. Ceotto-Vigoder, S.L. Marques, I.N. Santos, M.D. Alves, E.S. Barrias, A. Potter, D.S. Alviano, M.C. Bastos, Nisin and lysostaphin activity against preformed biofilm of *Staphylococcus aureus* involved in bovine mastitis, J. Appl. Microbiol. 121 (1) (2016) 101–114, https://doi.org/10.1111/jam.13136. Epub 2016 May 13.
[38] C. Velazquez-Suarez, R. Cebrian, C. Gasca-Capote, A. Sorlózano-Puerto, J. Gutiérrez-Fernández, M. Martínez-Bueno, M. Maqueda, E. Valdivia, Antimicrobial activity of the circular bacteriocin AS-48 against clinical multidrug-resistant *Staphylococcus aureus*, Antibiotics (Basel) 10 (8) (2021) 925, https://doi.org/10.3390/antibiotics10080925.
[39] V.K. Juneja, Predictive model for the combined effect of temperature, sodium lactate, and sodium diacetate on the heat resistance of *Listeria monocytogenes* in beef, J. Food Prot. 66 (5) (2003) 804–811, https://doi.org/10.4315/0362-028x-66.5.804.
[40] A. Baños, J.J. Ariza, C. Nuñez, L. Gil-Martínez, J.D. García-López, M. Martínez-Bueno, E. Valdivia, Effects of *Enterococcus faecalis* UGRA10 and the enterocin AS-48 against the fish pathogen *Lactococcus garvieae*. Studies *in vitro* and *in vivo*, Food. Microbiol. 77 (2019) 69–77, https://doi.org/10.1016/j.fm.2018.08.002. Epub 2018 Aug 10.
[41] F.I. Sonbol, A.A. Abdel Aziz, T.E. El-Banna, O.M. Al-Fakhrany, Antimicrobial activity of bacteriocins produced by *Enterococcus* isolates recovered from Egyptian homemade dairy products against some foodborne pathogens, Int. Microbiol. 23 (4) (2020) 533–547, https://doi.org/10.1007/s10123-020-00127-z. Epub 2020 Apr 18.
[42] R.E. Wirawan, K.M. Swanson, T. Kleffmann, R.W. Jack, J.R. Tagg, Uberolysin: a novel cyclic bacteriocin produced by *Streptococcus uberis*, Microbiology 153 (5) (2007) 1619–1630, https://doi.org/10.1099/mic.0.2006/005967-0.
[43] R. Cebrián, S. Arévalo, S. Rubiño, S. Arias-Santiago, M.D. Rojo, M. Montalbán-López, M. Martínez-Bueno, E. Valdivia, M. Maqueda, Control of *Propionibacterium acnes* by natural antimicrobial substances: role of the bacteriocin AS-48 and lysozyme, Sci. Rep. 8 (1) (2018) 11766, https://doi.org/10.1038/s41598-018-29580-7.
[44] Y. Lu, H. Yan, X. Li, Y. Gu, X. Wang, Y. Yi, Y. Shan, B. Liu, Y. Zhou, X. Lü, Physicochemical properties and mode of action of a novel bacteriocin BM1122 with broad antibacterial spectrum produced by *Lactobacillus crustorum* MN047, J. Food Sci. 85 (5) (2020) 1523–1535, https://doi.org/10.1111/1750-3841.15131. Epub 2020 Apr 13.
[45] Y. Kawai, Y. Ishii, K. Arakawa, K. Uemura, B. Saitoh, J. Nishimura, H. Kitazawa, Y. Yamazaki, Y. Tateno, T. Itoh, Structural and functional differences in two cyclic bacteriocins with the same sequences produced by lactobacilli, Appl. Environ. Microbiol. 70 (5) (2004) 2906–2911, https://doi.org/10.1128/AEM.70.5.2906-2911.2004.
[46] X. Gong, L.A. Martin-Visscher, D. Nahirney, J.C. Vederas, M. Duszyk, The circular bacteriocin, carnocyclin A, forms anion-selective channels in lipid bilayers, Biochim. Biophys. Acta 1788 (9) (2009) 1797–1803, https://doi.org/10.1016/j.bbamem.2009.05.008.
[47] M.J. Grande Burgos, A.T. Kovács, A.M. Mirończuk, H. Abriouel, A. Gálvez, O.P. Kuipers, Response of *Bacillus cereus* ATCC 14579 to challenges with sublethal concentrations of enterocin AS-48, BMC Microbiol. 9 (2009) 227, https://doi.org/10.1186/1471-2180-9-227.
[48] Y. Liu, T. Fang, Y. Suo, S. Gao, G.M. Baranzoni, C.M. Armstrong, Transcriptomics of *Listeria monocytogenes* treated with olive leaf extract, Front. Microbiol. 12 (2021) 782116, https://doi.org/10.3389/fmicb.2021.782116.
[49] C. Melian, P. Castellano, F. Segli, L.M. Mendoza, G.M. Vignolo, Proteomic analysis of *Listeria monocytogenes* FBUNT during biofilm formation at 10°C in response to Lactocin AL705, Front. Microbiol. 12 (2021) 604126, https://doi.org/10.3389/fmicb.